

CHAPTER VI

DISCUSSIONS AND CONCLUSIONS

In this chapter, we will discuss about the results that we obtained from the previous chapter and then make conclusions and comments.

Discussions and Results

In the previous chapter, we applied the Lorenz model to the atmospheric circulation. This model is based on the quasi-geostrophic vorticity equation which is a simplified equation. The one important assumption is that the vertical vorticity is omitted and Coriolis parameter replaced by a constant value (f_0). This assumption will be true in the case of the vertical vorticity is less than the Coriolis parameter (f), that is better in the mid-latitude region. We have calculated equilibrium states of the truncated spectral model for some special cases of the atmospheric circulation.

We first discuss about the equilibrium states of a conservative flow as shown in Fig. 5.2 as follows:

In Fig. 5.2a, the streamfunction spreads from the western domain to the eastern domain and no circulation occurs.

In Fig. 5.2b and Fig. 5.2c, the streamfunction patterns are complicate, because there are some circulations occurring. Fig. 5.2b shows that there are three circulations occurring. One is a negative circulation centered at about (3.14, 0.60), and the others are positive circulations centered at about (1.57, 2.50) and (4.71, 2.50). Fig. 5.2c shows that there are three circulations occurring. One is a negative circulation centered at about

(3.14, 1.26), and the others are positive circulations centered at about (1.57, 1.88) and (4.71, 1.88).

By the stability consideration of equilibrium states for a conservative flow, we obtain that

- (i) the equilibrium states (0.100000, 0, 0) and (0.100000, 0.055989, 0) are stable equilibrium states, since all three eigenvalues of the stability M_0 in Eq.(5.17) have non-positive real parts.
- (ii) the equilibrium states (0.100000, 0.223957, 0), (0.100000, 0.280026, 0), (0.100000, 0.336015, 0), (0.100000, 0.392004, 0) and (0.100000, 0.447993, 0) are unstable equilibrium states, since one of three eigenvalues of the stability M_0 in Eq.(5.17) have positive real part.

The results show that when h_0/H increases, the asymptotic stability of (X_0, Y_0, Z_0) gives way to instability.

We then discuss about the equilibrium states of a topographically and thermally driven flow as shown in Fig. 5.3 and Fig. 5.4 as follows:

In Fig. 5.3a and Fig. 5.4a, there are three circulations occurring in each case. Two of these are negative, and the other one is positive.

In Fig. 5.3b and Fig. 5.4b, there are three circulations occurring in each case. Two of these are positive, and the other one is negative.

Fig. 5.3c and Fig. 5.4c show the inflow of streamfunctions from the western domain to the eastern domain. In Fig. 5.3c, there are some parts of streamfunctions return back to the western domain, so that some positive circulations occur.

We now consider the stability of equilibrium states of a topographically and thermally driven flow as shown in Table 5.2 - 5.3. We obtain that

- (i) when Ψ_1^* is small, there is only one equilibrium state. Since all three eigenvalues of the stability M_0 in Eq.(5.21) have negative real parts, so that the equilibrium state is stable.

- (ii) when Ψ_1^* is larger, there are three equilibrium states; two of these are stable, the other is unstable.

This result shows that when Ψ_1^* increases, the behaviour of our system gives way to be complicate.

In the special case for $\phi_0 = 45^\circ$, $L/a = 1/4$, $n = 2$, $h_0/H = 0.05$, $k = 10^{-2}$, and $\Psi_1^* = 0.20$, Table 5.2 gives two stable equilibrium states (0.027221, -0.046929, -0.012219) and (0.181164, 0.041285, -0.001332), and one unstable equilibrium state (0.080004, 0.068762, -0.008486). From the numerical results as shown in Table 5.4 - Table 5.9 in the previous chapter, the phase portrait of the flow are shown in Fig. 6.1 - Fig. 6.6.

We also introduce the Liapunov exponent as quantitative measure to characterize the chaotic behaviour of the system [Schuster 1984].

Rewrite the solutions of Eqs.(5.24) in the form

$$\begin{aligned} X_N &= X(t_0 + N\Delta t), \\ Y_N &= Y(t_0 + N\Delta t), \\ Z_N &= Z(t_0 + N\Delta t), \end{aligned} \tag{6.1}$$

where N is the number of iterations,

(X_N, Y_N, Z_N) is the state of the flow at the time $t = t_0 + N\Delta t$ when an initial condition (X_0, Y_0, Z_0) has been chosen.

Likewise, when an initial condition $(X_0 + \epsilon, Y_0 + \epsilon, Z_0 + \epsilon)$ has been chosen, the solutions of Eqs.(5.24) can be written in the form

$$\begin{aligned}
X_N^* &= X^*(t_0 + N\Delta t) , \\
Y_N^* &= Y^*(t_0 + N\Delta t) , \\
Z_N^* &= Z^*(t_0 + N\Delta t) ,
\end{aligned} \tag{6.2}$$

where

(X_N^*, Y_N^*, Z_N^*) is the state of the flow at the time $t = t_0 + N\Delta t$ when an initial condition $(X_0 + \varepsilon, Y_0 + \varepsilon, Z_0 + \varepsilon)$ has been chosen; in this study we choose $\varepsilon = 10^{-6}$.

By the definition of the Liapunov exponent [Schuster 1984], the Liapunov exponents of (X_0, Y_0, Z_0) are

$$\begin{aligned}
\lambda_X(X_0, Y_0, Z_0) &= \lim_{N \rightarrow \infty} \lim_{\varepsilon \rightarrow 0} \frac{1}{N} \ln \left| \frac{X_N^* - X_N}{\varepsilon} \right| , \\
\lambda_Y(X_0, Y_0, Z_0) &= \lim_{N \rightarrow \infty} \lim_{\varepsilon \rightarrow 0} \frac{1}{N} \ln \left| \frac{Y_N^* - Y_N}{\varepsilon} \right| , \\
\lambda_Z(X_0, Y_0, Z_0) &= \lim_{N \rightarrow \infty} \lim_{\varepsilon \rightarrow 0} \frac{1}{N} \ln \left| \frac{Z_N^* - Z_N}{\varepsilon} \right| ,
\end{aligned} \tag{6.3}$$

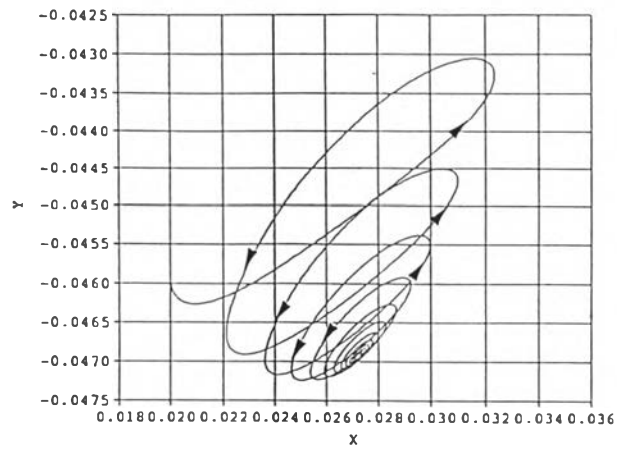
where

$\lambda_X(X_0, Y_0, Z_0)$ is the Liapunov exponent in X-component,

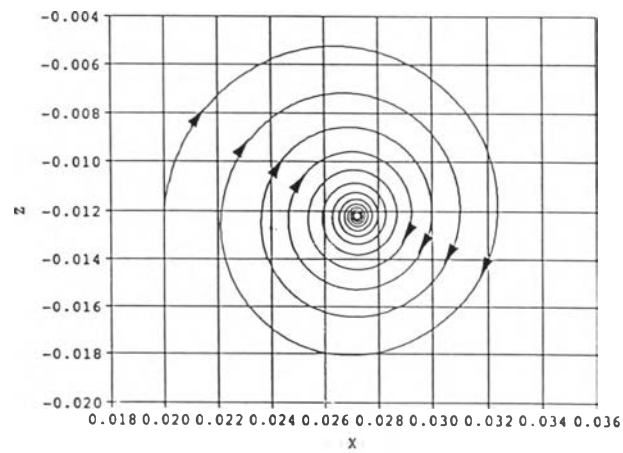
$\lambda_Y(X_0, Y_0, Z_0)$ is the Liapunov exponent in Y-component,

$\lambda_Z(X_0, Y_0, Z_0)$ is the Liapunov exponent in Z-component.

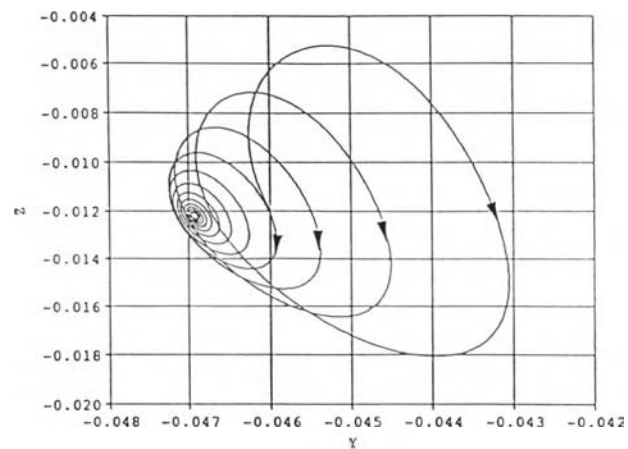
If the Liapunov exponents are all negative the system will be considered as a *normally system*, on the other hand if one of the Liapunov exponents is positive the system must be considered as a *chaotic system*. The calculations of the Liapunov exponents are shown in Fig. 6.7 - Fig. 6.9.



(a)

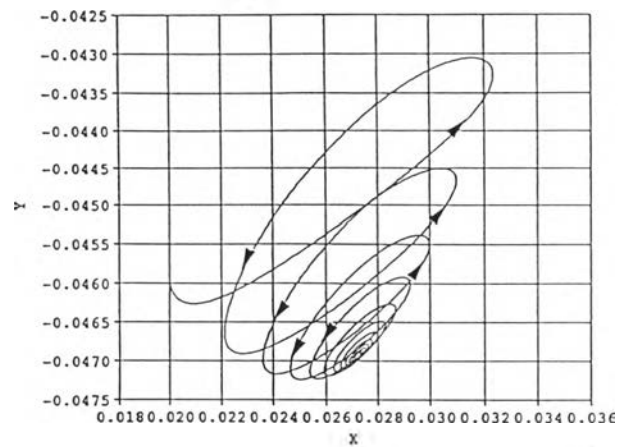


(b)

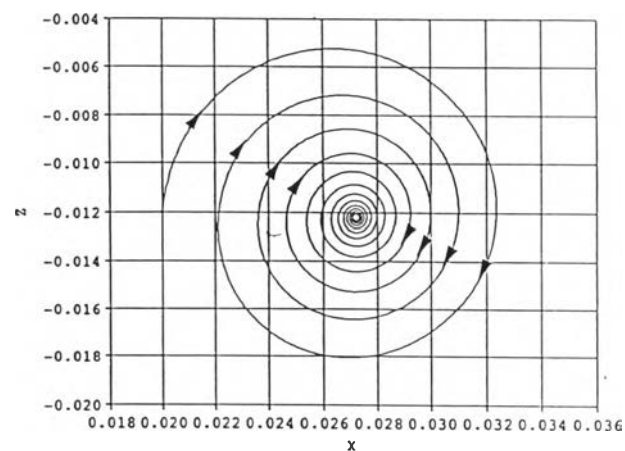


(c)

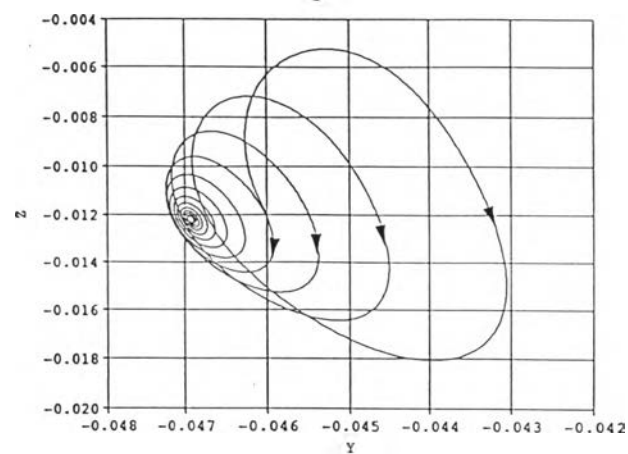
Figure 6.1 Phase portrait of a topographically and thermally driven flow for $\phi_0 = 45^\circ$, $L/a = 1/4$, $n = 2$, $h_0/H = 0.05$, $k = 10^{-2}$, and $\psi_1^* = 0.20$ with the initial condition $(0.020000, -0.046000, -0.012000)$ projected onto;
 (a) XY-plane (b) XZ-plane (c) YZ-plane



(a)

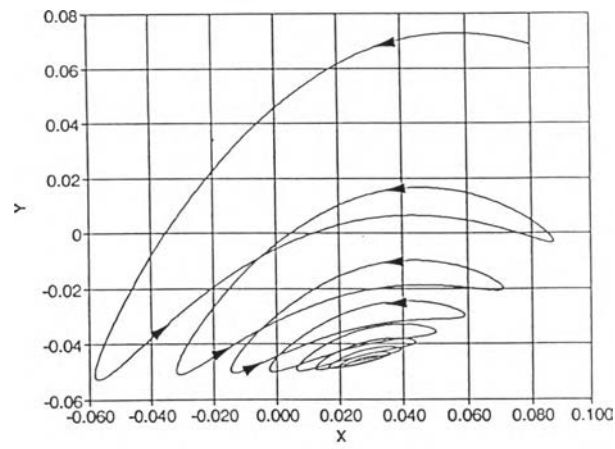


(b)

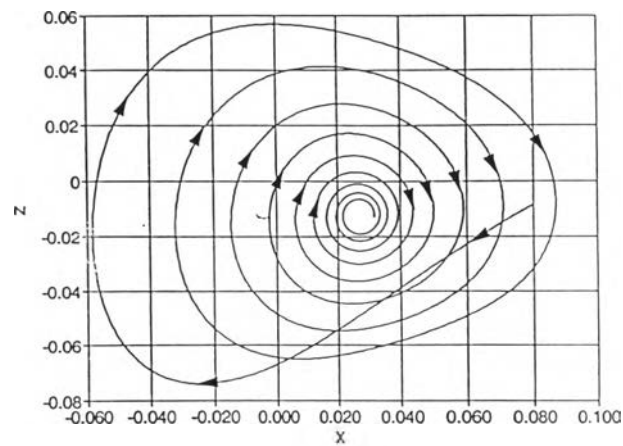


(c)

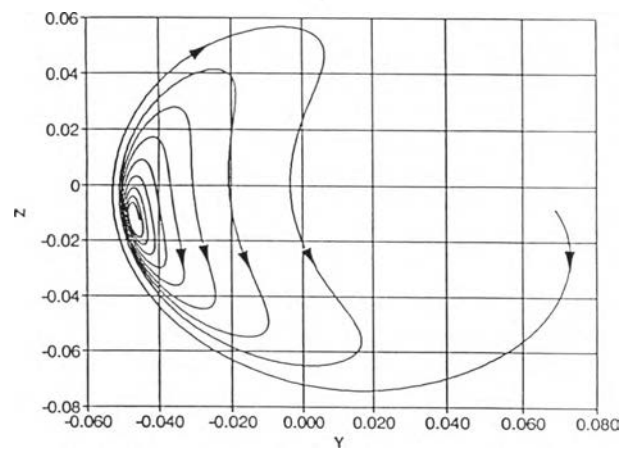
Figure 6.2 Phase portrait of a topographically and thermally driven flow for $\phi_0 = 45^\circ$, $L/a = 1/4$, $n = 2$, $h_0/H = 0.05$, $k = 10^{-2}$, and $\psi_1^* = 0.20$ with the initial condition $(0.020001, -0.046001, -0.012001)$ projected onto;
 (a) XY-plane (b) XZ-plane (c) YZ-plane



(a)

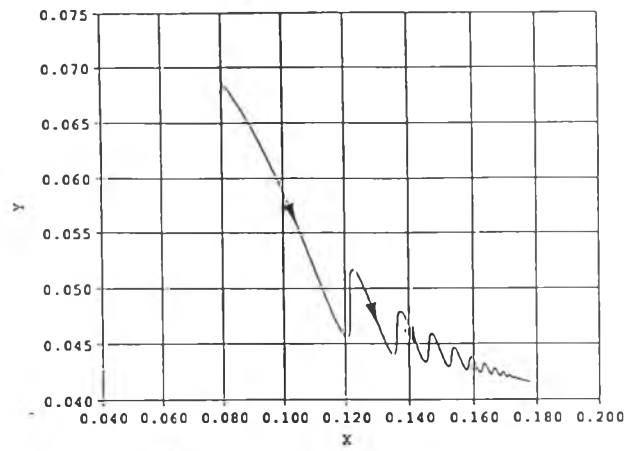


(b)

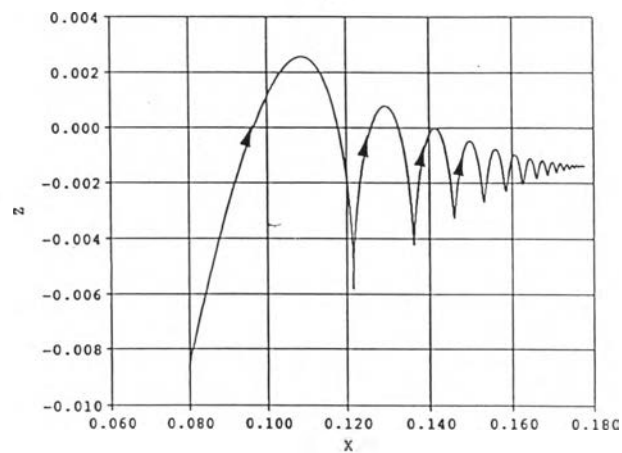


(c)

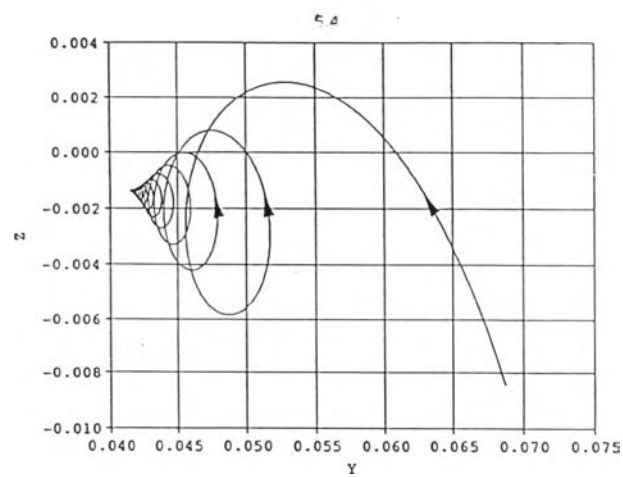
Figure 6.3 Phase portrait of a topographically and thermally driven flow for $\phi_0 = 45^\circ$, $L/a = 1/4$, $n = 2$, $h_0/H = 0.05$, $k = 10^{-2}$, and $\Psi_1^* = 0.20$ with the initial condition $(0.080000, 0.068762, -0.008486)$ projected onto; (a) XY-plane (b) XZ-plane (c) YZ-plane



(a)

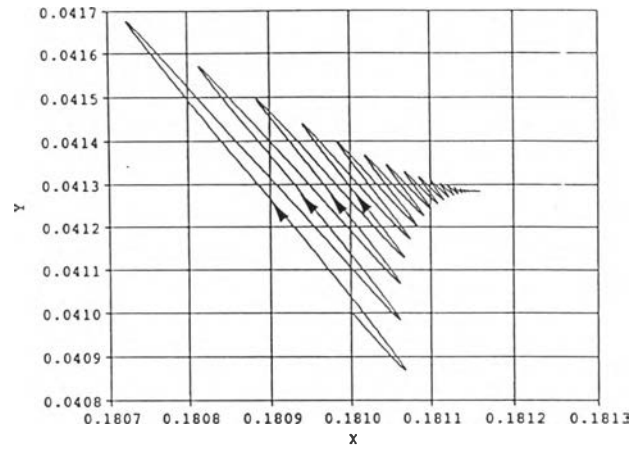


(b)

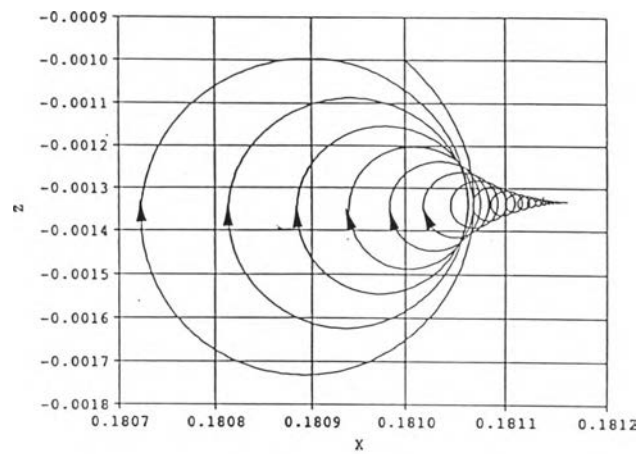


(c)

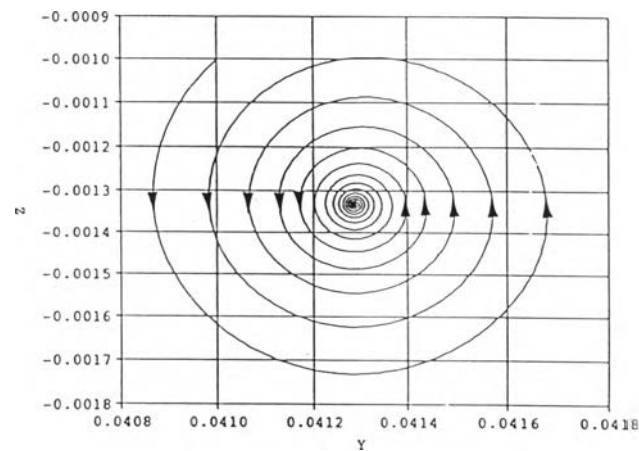
Figure 6.4 Phase portrait of a topographically and thermally driven flow for $\phi_0 = 45^\circ$, $L/a = 1/4$, $n = 2$, $h_0/H = 0.05$, $k = 10^{-2}$, and $\psi_1^* = 0.20$ with the initial condition $(0.080001, 0.068763, -0.008485)$ projected onto; (a) XY-plane (b) XZ-plane (c) YZ-plane



(a)

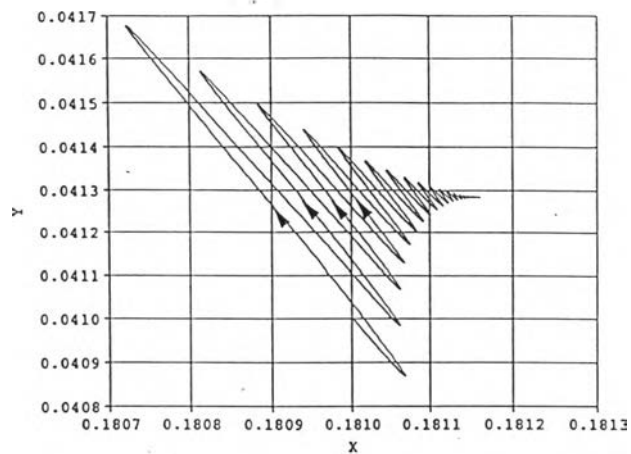


(b)

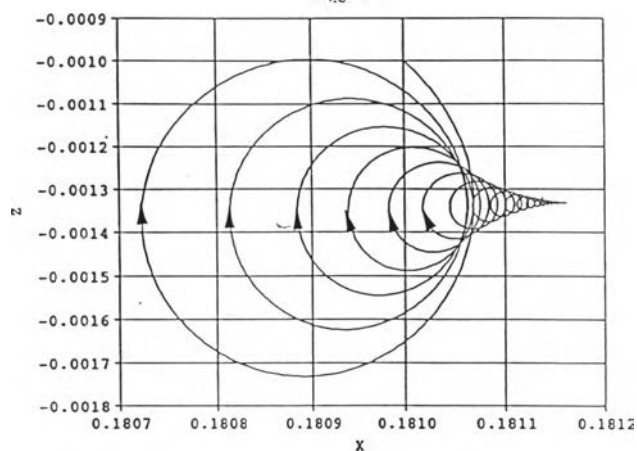


(c)

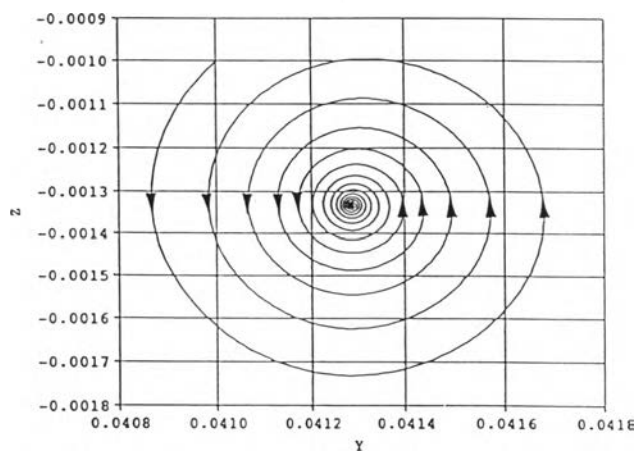
Figure 6.5 Phase portrait of a topographically and thermally driven flow for $\phi_0 = 45^\circ$, $L/a = 1/4$, $n = 2$, $h_0/H = 0.05$, $k = 10^{-2}$, and $\psi_1^* = 0.20$ with the initial condition $(0.181000, 0.041000, -0.001000)$ projected onto;
 (a) XY-plane (b) XZ-plane (c) YZ-plane



(a)

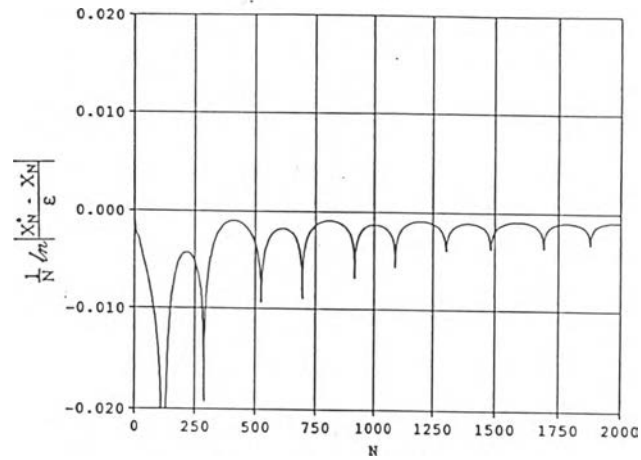


(b)

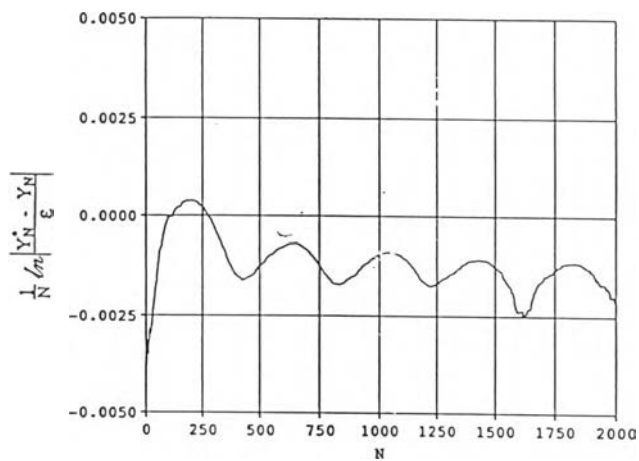


(c)

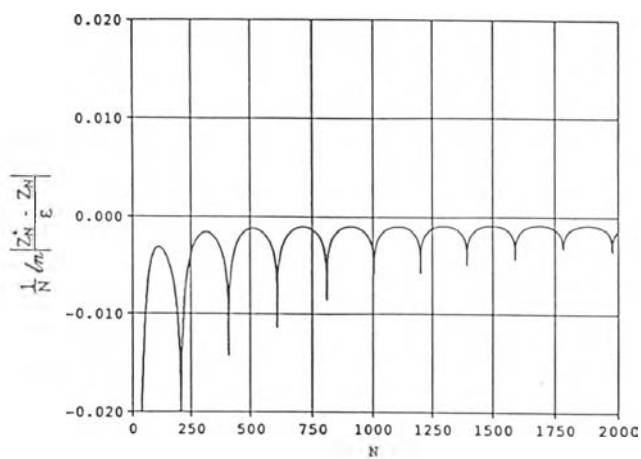
Figure 6.6 Phase portrait of a topographically and thermally driven flow for $\phi_0 = 45^\circ$, $L/a = 1/4$, $n = 2$, $h_0/H = 0.05$, $k = 10^{-2}$, and $\psi_1^* = 0.20$ with the initial condition $(0.181001, 0.041001, -0.001001)$ projected onto; (a) XY-plane (b) XZ-plane (c) YZ-plane



(a)



(b)



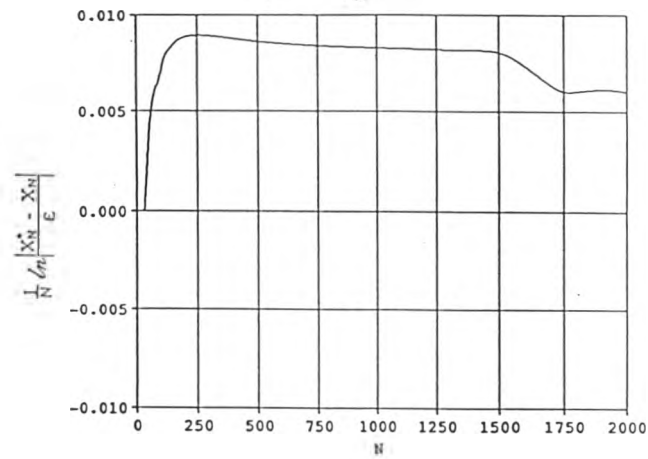
(c)

Figure 6.7 Liapunov exponent of the state $(0.020000, -0.046000, -0.012000)$ of a topographically and thermally driven flow for $\phi_0 = 45^\circ$, $L/a = 1/4$, $n = 2$, $h_0/H = 0.05$, $k = 10^{-2}$, and $\psi_1^* = 0.20$;

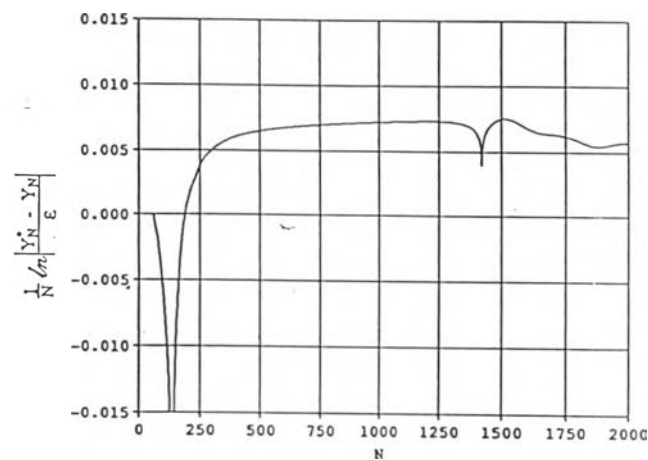
(a) in X-component

(b) in Y-component

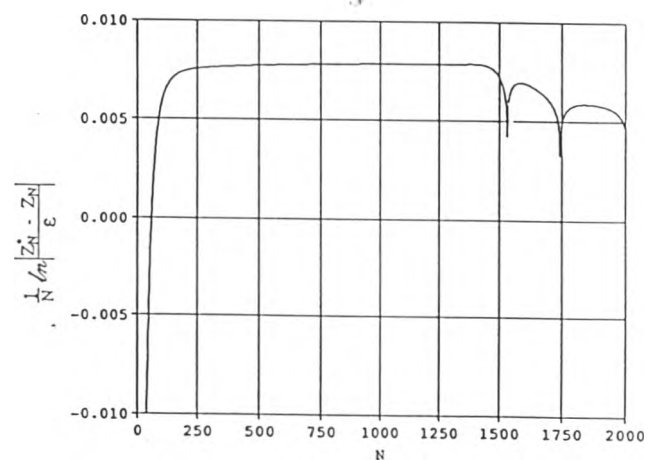
(c) in Z-component



(a)



(b)



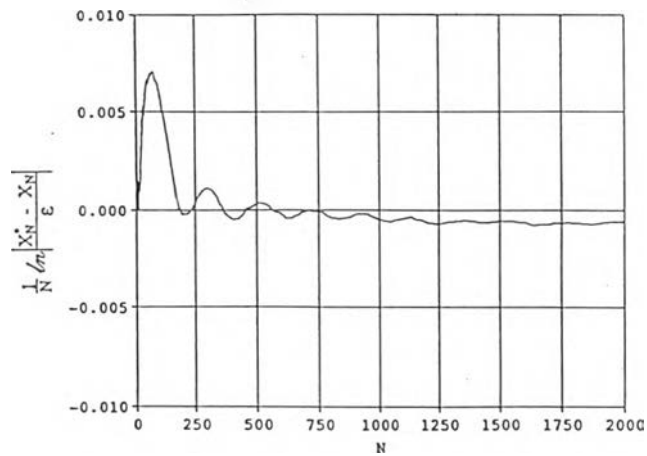
(c)

Figure 6.8 Liapunov exponent of the state $(0.080000, 0.068762, -0.008486)$ of a topographically and thermally driven flow for $\phi_0 = 45^\circ$, $L/a = 1/4$, $n = 2$, $h_0/H = 0.05$, $k = 10^{-2}$, and $\psi_1^* = 0.20$;

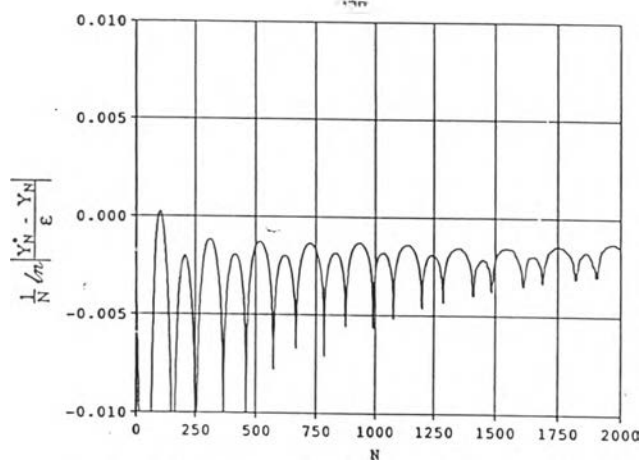
(a) in X-component

(b) in Y-component

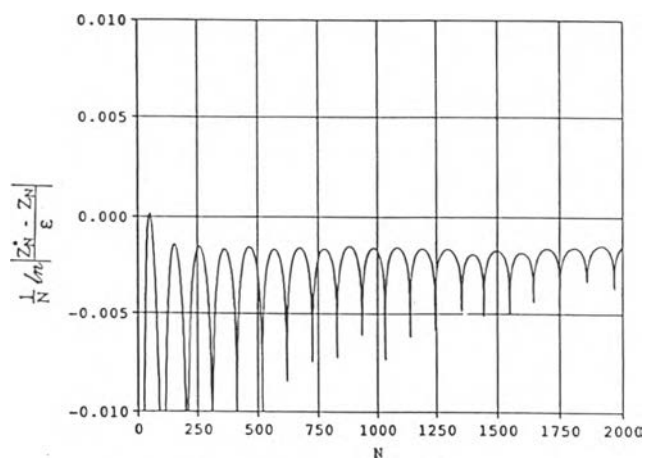
(c) in Z-component



(a)



(b)



(c)

Figure 6.9 Liapunov exponent of the state $(0.181000, 0.041000, -0.001000)$ of a topographically and thermally driven flow for $\phi_0 = 45^\circ$, $L/a = 1/4$, $n = 2$, $h_0/H = 0.05$, $k = 10^{-2}$, and $\Psi_1^* = 0.20$;

(a) in X-component (b) in Y-component (c) in Z-component

Fig. 6.1 and Fig. 6.2 show the phase flow near an equilibrium state (0.027221, -0.046929, -0.012219). The solutions have converged to this equilibrium state. Since eigenvalues of the stability matrix M_0 are $\lambda = -0.015, -0.007 \pm 0.156 i$, this equilibrium state is a stable spiral point and a damped oscillation occurred. Moreover, since the Liapunov exponent of the state (0.020000, -0.046000, -0.012000) of the flow as shown in Fig. 6.7 are all negative, hence that the behaviour of our system near the equilibrium state (0.027221, -0.046929, -0.012219) is not sensitive to the initial condition.

Fig. 6.5 and Fig. 6.6 show the phase flow near an equilibrium state (0.181164, 0.041285, -0.001332). The solutions have converged to this equilibrium state. Since eigenvalues of the stability matrix M_0 are $\lambda = -0.009, -0.011 \pm 0.305 i$, so that this equilibrium state is a stable spiral point and a damped oscillation occurred. Moreover, since the Liapunov exponent of the state (0.181000, 0.041000, -0.001000) of the flow as shown in Fig. 6.9 are all negative, hence that the behaviour of our system near the equilibrium state (0.181164, 0.041285, -0.001332) is not sensitive to the initial condition.

Fig. 6.3 and Fig. 6.4 show the phase flow near an equilibrium state (0.080004, 0.068762, -0.008486). Since eigenvalues of the stability matrix are $\lambda = 0.079$, and $-0.054 \pm 0.022 i$, so that this equilibrium state is a unstable spiral point. In Fig. 6.3, the solution have converged to a stationary point, while in Fig. 6.4, the solutions have diverged. The results, in Fig. 6.3 and in Fig. 6.4, are far different though the initial conditions are tiny different - i.e. the difference of initial conditions equals (0.000001, 0.000001, 0.000001). Moreover, since the Liapunov exponent of the state (0.080000, 0.068762, -0.008486) of the flow as shown in Fig. 6.8 are positive, hence that the behaviour of our system near the equilibrium state (0.080004, 0.068762, -0.008486) is sensitive to the initial condition.. These results show that tiny difference in initial conditions can lead to far different values after a period of time. This sensitive

dependence led us to consider the system as a *chaotic system*, so that we can not do a very-long-range forecasting.

Conclusions and Comments

From this study, when we applied the Lorenz model to the quasi-geostrophic vorticity of the atmospheric circulation, the system will be treated as a finite system of ordinary differential equations. We have studied in detail the properties of its solutions. Our principal results concern the stability or instability of solutions. We have obtained numerical solutions of a system of three ordinary differential equations designed to represent a topographically and thermally driven flow for $\phi_0 = 45^\circ$, $L/a = 1/4$, $n = 2$, $h_0/H = 0.05$, $k = 10^{-2}$, and $\psi_1^* = 0.20$. The equations possess three steady-state solutions. One of these is found to be unstable. From the numerical results, the system has been treated as a chaotic system because of the sensitive dependence. This result shows that our model is a reasonable one, although it can not indicate the acceptable forecasts because it is a highly truncated spectral model. One must eventually deal with more accurate models by using a fairly large number of degrees of freedom.